

# A systematic study of the superdeformation of Pb isotopes with relativistic mean field theory

Jian-You Guo,<sup>1,\*</sup> Zong-Qiang Sheng,<sup>2</sup> and Xiang-Zheng Fang<sup>1</sup>

<sup>1</sup>*School of physics and material science, Anhui university, Hefei 230039, P.R. China*

<sup>2</sup>*Department of mathematics and physics, Anhui University of Science and Technology, Huainan 232001, P.R. China*

The microscopically constrained relativistic mean field theory is used to investigate the superdeformation for Pb isotopes. The calculations show that there exists a clear superdeformed minimum in the potential energy surfaces with four different interactions NL3, PK1, TM1 and NLSH. The excitation energy, deformation and depth of well in the superdeformed minimum are comparable for four different interactions. Furthermore the trend for the change of the superdeformed excitation energy with neutron number is correctly reproduced. The calculated two-neutron separation energy in the ground state and superdeformed minimum together with their differences are in agreement with the data available. The larger energy difference appearing in superdeformed minimum reflects a lower average level density at superdeformations for Pb isotopes.

PACS numbers: 21.10.-k, 21.60.Jz, 21.10.Dr

Superdeformation(SD) of atomic nuclei is one of the most interesting topics of nuclear structure studies. Over the past two decades, many rotational bands associated with SD shapes have been observed in several regions of the nuclear chart [1], with 85 SD bands observed in nuclei with  $79 < Z < 84$  (the  $A \sim 190$  region) alone, where an impressive number of results has been obtained. Unfortunately, despite the rather large amount of experimental information on SD bands, there are still a number of very interesting properties, which have not yet been measured. The characteristic examples are the spin, parity and excitation energy relative to the ground state of the SD bands. The difficulty lies with observing the very weak discrete transitions which link SD levels with levels of normal deformation (ND levels). Until now, only several SD bands have been identified to exist the transitions from SD levels to ND levels in the  $A \sim 190$  region: two bands in  $^{194}\text{Hg}$  [2, 3], and one band in each of  $^{194}\text{Pb}$  [4, 5],  $^{192}\text{Pb}$  [6], and  $^{191}\text{Hg}$  [7]. Less precise measurements have been achieved in  $^{192}\text{Hg}$  [8] and  $^{195}\text{Pb}$  [9] following analysis of the quasi-continuum component of the decay. Recently, the measurement of the excitation energy of the yrast (lowest energy for a given spin) SD band in  $^{196}\text{Pb}$  is reported [10], together with earlier measurements of the excitation energies of SD states in  $^{194}\text{Pb}$  and  $^{192}\text{Pb}$ , allows a systematic study of the energy of the SD well in a single isotope chain. Many theoretical models have been employed to study these superdeformed states of atomic nuclei. The Strutinsky method with a Woods-Saxon potential [11], the Hartree-Fock-Bogoliubov method with different mean field parameterizations [12, 13, 14], and the cluster model [15] have provided the predictions on the excitation energy of SD bands, where a gross trend of decreasing energy with decreasing neutron number is obtained for Pb isotopes, but the absolute energies as well as their differences are not consistently reproduced by these models as the analysis in Ref.[10]. Considering that the excitation energy and the well depth of the SD

minimum are amongst the most important factors which affect the decay of the SD bands to the ground state, the relativistic mean field (RMF) theory [16] has also been recently applied to estimate the excitation energies and depths of well for SD bands. The excitation energies and depths of well in the SD minima of  $^{194}\text{Hg}$  and  $^{194}\text{Pb}$  have been predicted in considerable agreement as compared with experiment [17]. However, a systematic study of the energy of the SD well in a single isotope chain presented in Ref.[10] with the nonrelativistic theories, has not been performed in a relativistic framework. In recent years, the RMF theory has gained considerable success in describing many nuclear phenomena for the stable nuclei [18, 19] as well as nuclei even far from stability [20]. It has been shown that the RMF theory can reproduce better the nuclear saturation properties (the Coester line) in nuclear matter [21], present a new explanation for the neutron halo [22] and predict a new phenomenon — giant neutron halos in heavy nuclei close to the neutron drip line [23], give naturally the spin-orbit potential, the origin of the pseudospin symmetry [24, 25] as a relativistic symmetry [26, 27, 28] and spin symmetry in the anti-nucleon spectrum [29], and present good description for the magnetic rotation [30], the collective multipole excitations [31], the identical bands in superdeformed nuclei [32], and the excitation energies relative to the ground of SD bands [17]. Hence, here we will report a systematic investigation of SD states for Pb isotopes in the microscopic quadruple constrained RMF theory with pairing treated by the BCS method, and show an excellent empirical manifestations of this SD structure in Pb isotopes including the evolution of the excitation energy, depth of well, deformation, and shell structure as well as the comparison with the ND states.

The starting point of RMF theory is a standard Lagrangian density where nucleons are described as Dirac particles which interact via the exchange of various mesons including the isoscalar-scalar  $\sigma$  meson, the

isoscalar-vector  $\omega$  meson and the isovector-vector  $\rho$  meson. The effective Lagrangian density considered is written in the form:

$$\begin{aligned} \mathcal{L} = & \bar{\psi}_i (i\partial\!\!\!/ - M) \psi_i + \frac{1}{2} \partial_\mu \sigma \partial^\mu \sigma - U(\sigma) - g_\sigma \bar{\psi}_i \sigma \psi_i \\ & - \frac{1}{4} \Omega_{\mu\nu} \Omega^{\mu\nu} + \frac{1}{2} m_\omega^2 \omega_\mu \omega^\mu - g_\omega \bar{\psi}_i \boldsymbol{\psi} \psi_i \\ & - \frac{1}{4} \vec{R}_{\mu\nu} \vec{R}^{\mu\nu} + \frac{1}{2} m_\rho^2 \vec{\rho}_\mu \vec{\rho}^\mu - g_\rho \bar{\psi}_i \vec{\boldsymbol{\rho}} \vec{\boldsymbol{\tau}} \psi_i \\ & - \frac{1}{4} F_{\mu\nu} F^{\mu\nu} - e \bar{\psi}_i \frac{1 - \tau_3}{2} \mathbf{A} \psi_i, \end{aligned} \quad (1)$$

where  $\bar{\psi} = \psi^\dagger \gamma^0$  and  $\psi$  is the Dirac spinor. Other symbols have their usual meanings.

The Dirac equation for the nucleons and the Klein-Gordon type equations for the mesons and the photon are given by the variational principle and can be solved by expanding the wavefunctions in terms of the eigenfunctions of a deformed axially symmetric harmonic-oscillator potential [33] or a Woods-Saxon potential [34]. The details can be also found in Ref. [19] and references therein.

The potential energy curve can be calculated microscopically by the constrained RMF theory. The binding energy at certain deformation value is obtained by constraining the quadrupole moment  $\langle Q_2 \rangle$  to a given value  $\mu_2$  in the expectation value of the Hamiltonian [35],

$$\langle H' \rangle = \langle H \rangle + \frac{1}{2} C_\mu (\langle Q_2 \rangle - \mu_2)^2, \quad (2)$$

where  $C_\mu$  is the constraint multiplier.

For the nuclei studied in this paper, the deformed harmonic oscillator basis is taken into account and the convergence of the numerical calculation on the binding energy and the deformation is very good. The converged deformations corresponding to different  $\mu_2$  are not sensitive to the deformation parameter  $\beta_0$  of the harmonic oscillator basis in a reasonable range due to the large basis. The different choices of  $\beta_0$  lead to different iteration numbers of the self-consistent calculation and different computational time. But physical quantities such as the binding energy and the deformation change very little. Thus the deformation parameter  $\beta_0$  of the harmonic oscillator basis is chosen near the expected deformation to obtain high accuracy and low computation time cost. By varying  $\mu_2$ , the binding energy at different deformation can be obtained. The pairing is considered by the constant gap approximation (BCS) in which the pairing gap is taken as  $12/\sqrt{A}$  for even number nucleons.

The calculated potential energy curves for  $^{190-204}\text{Pb}$  are exhibited respectively in the figures 1, 2, 3, and 4 for the interactions NL3 [36], PK1 [37], TM1 [38] and NLSH [39], in which the energy of the ground state is taken as a reference. The  $E_x$  and  $V$  are respectively the excitation energy and depth of well of the SD minimum as shown in the subfigure for  $^{196}\text{Pb}$ . Similar patterns are found for all the effective interactions. Most of the curves

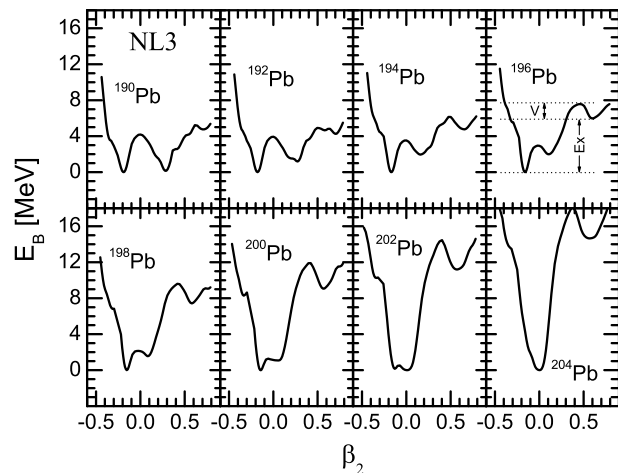


FIG. 1: The potential energy curves for  $^{190-204}\text{Pb}$  obtained by the constrained RMF theory with the interactions NL3, where the  $E_x$  and  $V$  represent respectively for the excitation energy relative to the ground state of superdeformed minimum and the depth of well of superdeformed minimum. The ground state binding energy is taken as a reference.

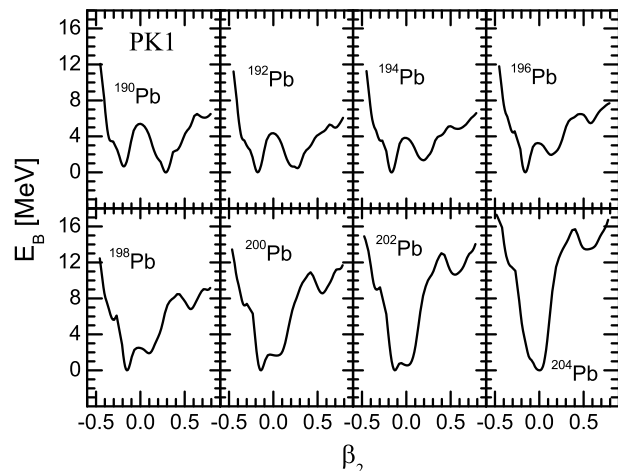


FIG. 2: The same as Fig. 1, but with PK1

display a clear SD minimum for the Pb isotopes, especially for the nuclei with more neutron number. For  $^{190,192}\text{Pb}$ , the calculated SD minimum is not very obvious, even disappears for the interactions NLSH. For  $^{190}\text{Pb}$ , the RMF theory predicts a considerable high excitation energy relative to the ground of SD bands and shallow well in the SD minimum in comparison with its neighboring nucleus  $^{192}\text{Pb}$ , which implies that it is difficult to come into being the stable SD state. For  $^{192}\text{Pb}$ , although the well is shallow, the excitation energy is relatively lower, which indicates that it is relatively easy to form the SD state as observed in experiment. Start from the  $^{194}\text{Pb}$ , the RMF theory predicts that the excitation energy increases with

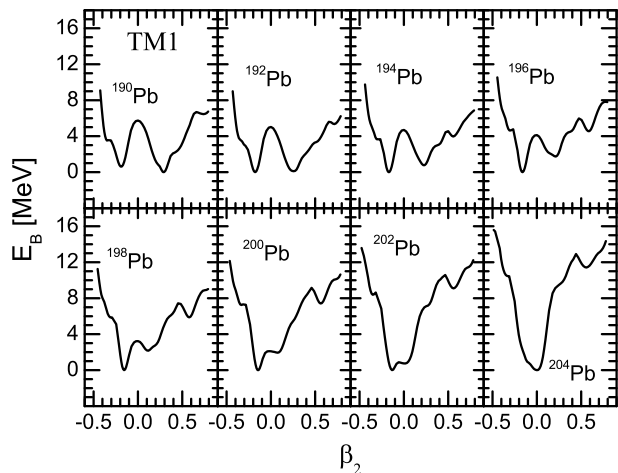


FIG. 3: The same as fig. 1, but with TM1

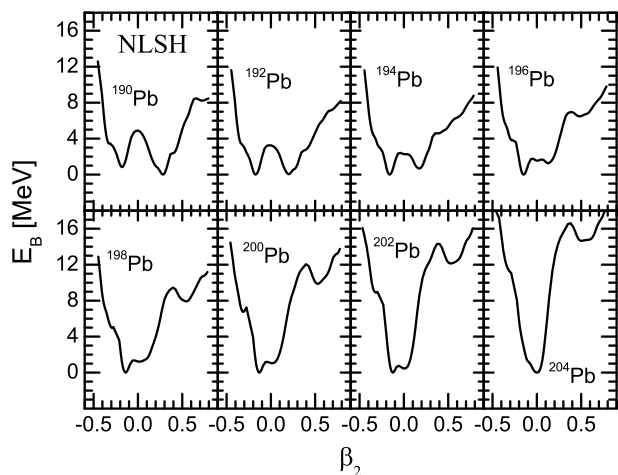


FIG. 4: The same as Fig. 1, but with NLSH

the increasing of the neutron number in company with the increasing of depth of well. So, the SD states can be still formed in these nuclei, which agrees the experimental observations. However for the  $N > 118$  nuclei, as the excitation energy is too high to make it difficult to excite the SD states. It may explain why only the SD nuclear states between  $N = 110$  and  $N = 116$  are observed in the Pb isotope chain. Besides the success in describing SD states, the RMF theory predicts an interesting feature in the ground state. The evolution of shape from the prolate to the oblate, and finally to the spherical shapes are found in the Pb isotope chain. From Figs.1-4, the ground state of  $^{190}\text{Pb}$  is exhibited a coexistence of the prolate and the oblate with about 5 MeV stiff barrier against deformation. Begin from  $^{190}\text{Pb}$ , the ground state gradually moves toward the oblate side with smaller and smaller deformation with the increasing of neutron num-

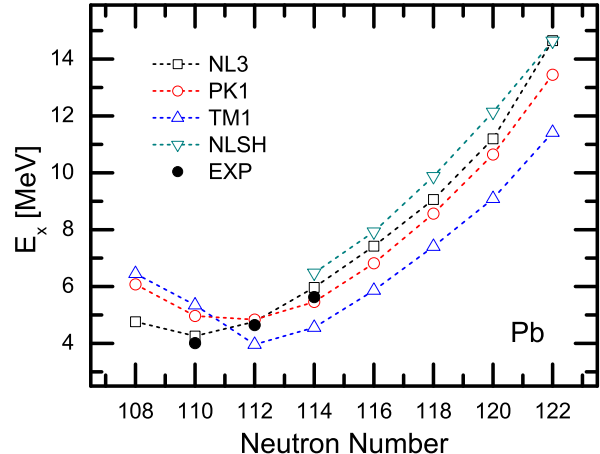


FIG. 5: The SD bandhead energies of Pb isotopes  $E_x$  as the functions of neutron number obtained by the constrained RMF calculations with the interactions NL3 (open squares), PK1 (open circles), TM1 (up triangles) and NLSH (down triangles) in comparison with the experimental data (filled circles).

ber. Finally well spherical  $^{204}\text{Pb}$  are seen.

In Fig.5, the calculated bandhead energies for SD bands as the functions of neutron number are displayed for Pb isotopes, where the open squares, open circles, up triangles, down triangles, and filled circles stand respectively for the RMF calculations with the interactions NL3, PK1, TM1, NLSH, and the data available [10]. First of all, trend for the change of the excitation energies with neutron number are correctly reproduced for all the effective interactions. Especially for the NL3, the calculated excitation energies are in excellent agreement with the data. The maximum deviation between theory and experiment is less than 0.34MeV. For the TM1 interactions, the excitation energy is overestimated for  $^{190}\text{Pb}$  and underestimated for  $^{192,194}\text{Pb}$ . A jump appears in  $^{194}\text{Pb}$ , which disagrees the experimental data. But the trend for the change of the excitation energies with neutron number is in accordance with the RMF predictions. For the PK1 interactions, except the excitation energy of  $^{192}\text{Pb}$  is overestimated, theoretical predictions is highly consistent with the experiment. For the NLSH interactions, the RMF theory fails to reproduce the SD minimum for  $^{192,194}\text{Pb}$ , but reproduce the SD minimum for  $^{196}\text{Pb}$ . In addition, the trend for the change of excitation energies with the neutron number is consistent with that in the other interactions. Compared the RMF calculations, the Strutinsky method with a Woods-Saxon potential [11], the Hartree-Fock-Bogoliubov method with different mean field parameterizations [12, 13, 14], and the cluster model[15] predict only a gross trend of decreasing energy with decreasing neutron number. The absolute energies and their differences are not consistently repro-

TABLE I: The quadruple deformation  $\beta_2$  and the depth of the superdeformed minimum  $V$  in the superdeformed states of  $^{190-204}\text{Pb}$  obtained by the constrained RMF theory with the interactions NL3, PK1, TM1 and NLSH.

$\beta_2$	NL3	PK1	TM1	NLSH
$^{190}\text{Pb}$	0.71848	0.71942	0.73864	
$^{192}\text{Pb}$	0.69986	0.69862	0.71772	
$^{194}\text{Pb}$	0.65808	0.57703	0.55686	
$^{196}\text{Pb}$	0.59984	0.57800	0.57885	0.47840
$^{198}\text{Pb}$	0.58028	0.56062	0.57834	0.53871
$^{200}\text{Pb}$	0.56225	0.55835	0.56068	0.53811
$^{202}\text{Pb}$	0.56170	0.54142	0.55967	0.52121
$^{204}\text{Pb}$	0.56161	0.54071	0.55935	0.50177
$V$	NL3	PK1	TM1	NLSH
$^{190}\text{Pb}$	0.46439	0.42181	0.22936	
$^{192}\text{Pb}$	0.66217	0.34837	0.25777	
$^{194}\text{Pb}$	1.37963	0.29612	0.59873	
$^{196}\text{Pb}$	1.60176	1.02856	1.41779	0.46892
$^{198}\text{Pb}$	2.17652	1.66011	1.56866	1.51712
$^{200}\text{Pb}$	2.83555	2.34135	1.75199	2.17761
$^{202}\text{Pb}$	3.25852	2.37082	1.48711	2.17321
$^{204}\text{Pb}$	3.51464	2.24769	1.49029	1.96709

duced by these model. It shows that the RMF theory gives a better description of the SD excitation energies for the Pb isotopes.

Besides the excitation energy, the deformation and well depth of SD minimum are another two important parameters which reflect the properties of the superdeformed states. In particular, the well depth affects the life time of the superdeformed states. In Table I, the quadruple deformation  $\beta_2$  and the depth of the superdeformed minimum  $V$  in the superdeformed states are listed respectively in the upper and lower panels for  $^{190-204}\text{Pb}$ . Except for several exceptions, the deformation in SD minima lies systemically between 0.5 and 0.7 for four different interactions NL3, PK1, TM1 and NLSH, which agrees the observation of superdeformed nuclei for excited states adopting ellipsoidal shapes with an axis ratio around 2:1 [1]. The RMF theory predicts for the height of the barrier is lower than 1 MeV for  $^{190,192}\text{Pb}$ , and higher than 1 MeV for  $^{196-214}\text{Pb}$  in all the interactions. For  $^{194}\text{Pb}$ , the estimated barriers are considerable different from different interactions.

Two-neutron separation energy defined as  $S_{2n}(Z, N) = E(Z, N) - E(Z, N - 2)$  is sensitive quantity to test a microscopic theory, where  $E(Z, N)$  is the binding energy of nucleus with proton number  $Z$  and neutron number  $N$ . In Table II, the two-neutron separation energies in the ground state  $S_{2n,\text{ND}}$  and SD minimum  $S_{2n,\text{SD}}$  are shown respectively in upper and lower panels for the Pb isotopes in comparison with the data[10, 40]. From there, it is found that the RMF calculations with four different interactions well reproduce the experimental data for  $S_{2n,\text{ND}}$ . The maximum deviation between the calcula-

TABLE II: Two-neutron separation energy in the ground state and superdeformation minimum obtained by the constrained RMF theory with the interactions NL3, PK1, TM1 and NLSH, in comparison with data available

N	$S_{2n,\text{ND}}$ [MeV]				EXP
	NL3	PK1	TM1	NLSH	
110	17.862	16.915	16.716	17.984	18.400
112	17.537	17.207	17.135	17.444	17.810
114	17.173	16.885	16.636	17.255	17.320
116	16.739	16.440	16.124	16.899	16.820
118	16.287	16.050	15.595	16.652	16.295
120	15.709	15.241	14.886	15.150	15.837
122	16.360	15.287	14.927	15.611	15.318
N	$S_{2n,\text{SD}}$ [MeV]				EXP
	NL3	PK1	TM1	NLSH	
110	18.364	18.025	17.908		
112	17.031	17.334	18.436		17.16(4)
114	15.968	16.266	16.037		16.31(4)
116	15.287	15.081	14.820	15.499	
118	14.648	14.303	14.051	14.653	
120	13.574	13.161	13.202	13.361	
122	12.906	12.484	12.601	12.637	

TABLE III: Two-neutron separation energy difference in the ground state and superdeformation minimum obtained by the constrained RMF theory with the interactions NL3, PK1, TM1 and NLSH, in comparison with data available

N	$\Delta S_{2n,\text{ND}}$ [MeV]				EXP
	NL3	PK1	TM1	NLSH	
110	0.325	-0.292	-0.419	0.540	0.590
112	0.364	0.322	0.499	0.189	0.490
114	0.434	0.445	0.512	0.356	0.500
116	0.452	0.390	0.529	0.247	0.525
118	0.578	0.809	0.709	1.502	0.458
120	-0.651	-0.046	-0.041	-0.461	0.519
N	$\Delta S_{2n,\text{SD}}$ [MeV]				EXP
	NL3	PK1	TM1	NLSH	
110	1.333	0.691	-0.528		
112	1.063	1.068	2.399		0.85(8)
114	0.681	1.185	1.217		
116	0.639	0.778	0.769	0.846	
118	1.074	1.142	0.849	1.292	
120	0.668	0.677	0.601	0.724	

tions and data is less than 1.7 MeV, especially for the NL3, the deviations is within 1 MeV. For  $S_{2n,\text{SD}}$ , the calculations with four different interactions are comparable and close to the data available. Both the calculations and experiment show that the  $S_{2n,\text{ND}}$  and  $S_{2n,\text{SD}}$  vary smoothly with the neutron number. No sharp drop in the binding energy is seen from the  $S_{2n}$ , which indicates no significant shell gap appearing in the Pb isotope chain whether the ground state or SD states.

In order to reveal further the detailed information on shell structure, the two-neutron separation energy differences  $\Delta S_{2n}(Z, N) = S(Z, N) - S(Z, N + 2)$  are presented

in Table III, where the  $\Delta S_{2n,ND}$  and  $\Delta S_{2n,SD}$  represent respectively for those in the ground state and superdeformed minimum with the data for comparison[10, 40]. From the Table III, it is found that the experimental  $\Delta S_{2n,ND}$  changes typically around 0.5MeV, is well reproduced in the RMF calculations for all the interactions with several exceptions. Compared with the other interactions, the NL3 gives better agreement with experiment. Only the deviation is relatively large at  $^{204}\text{Pb}$ . Furthermore, the calculated  $\Delta S_{2n,ND}$  shows very little differences for these nuclei with neutron number from  $N = 112$  to  $N = 118$ , is consistent with experiment data, which suggests without a shell closure appearing at  $N = 112$  or  $N = 114$  predicted in other calculations. Compared with the ND states, the SD separation energies  $S_{2n}$  are significantly larger than the typical ND value of 0.5 MeV, possibly reflecting a lower average level density at superdeformations. In particular, the  $\Delta S_{2n,SD}$  presents a obvious difference for different nuclei. The  $\Delta S_{2n,SD}$  for these nuclei with  $N = 112, 114, 118$  is much larger than that for their neighboring nuclei, suggest a larger shell gap in these SD states of  $^{112,114,118}\text{Pb}$ .

In summary, the superdeformation in  $^{190-204}\text{Pb}$  is investigated by the microscopic quadruple constrained relativistic mean field theory with all the most used interactions, i.e., NL3, PK1, TM1 and NLSH. The calculations show a clear SD minimum at nearly all the potential energy curves for the Pb isotopes with similar patterns for all the effective interactions. Trend for the change of the excitation energies with neutron number are correctly reproduced. The calculated deformation in SD minima lies systemically between 0.5 and 0.7, is consistent with the observation of experiment. The two-neutron separation energies in the ground state and the SD minimum are well reproduced with varying smoothly with the neutron number. Compared with the ND states, the SD separation energies  $S_{2n}$  are significantly larger than the typical ND value of 0.5 MeV, possibly reflecting a lower average level density at superdeformations.

This work was partly supported by the National Natural Science Foundation of China under Grant No. 10475001, the Program for New Century Excellent Talents in University of China, and the Excellent Talents Foundation in University of Anhui Province in China.

---

\* Electronic address: jianyou@ahu.edu.cn

- [1] B. Singh, R. Zywina, and R. B. Firestone, Nuclear Data Sheets 97, 241 (2002).
- [2] T. L. Khoo, M. P. Carpenter, T. Lauritsen et al., Phys. Rev. Lett. 76, 1583 (1996).
- [3] G. Hackman, T. L. Khoo, M. P. Carpenter et al., Phys. Rev. Lett. 79, 4100 (1997).
- [4] A. Lopez-Martens, F. Hannachi, A. Korichi et al., Phys. Lett. B 380, 18 (1996).
- [5] K. Hauschild, L. A. Bernstein, J. A. Becker et al., Phys. Rev. C 55, 2819 (1997).
- [6] A. N. Wilson, G. D. Dracoulis, A. P. Byrne et al., Phys. Rev. Lett. 90, 142501 (2003).
- [7] S. Siem, P. Reiter, T. L. Khoo et al., Phys. Rev. C 70, 014303 (2004).
- [8] T. Lauritsen, T. L. Khoo, I. Ahmad et al., Phys. Rev. C 62, 044316 (2000).
- [9] M. S. Johnson, J. A. Cizewski, K. Y. Ding et al., Phys. Rev. C 71, 044310 (2005).
- [10] A. N. Wilson, A. K. Singh, H. Hübel, et al., Phys. Rev. Lett. 95, 182501 (2005).
- [11] W. Satula et al., Nucl. Phys. A529, 289 (1991).
- [12] S. J. Krieger et al., Nucl. Phys. A542, 43 (1992).
- [13] P.-H. Heenen, J. Dobaczewski, W. Nazarewicz et al., Phys. Rev. C 57, 1719 (1998).
- [14] J. Libert, M. Girod, and J.-P. Delaroche, Phys. Rev. C 60, 054301 (1999).
- [15] G. G. Adamian, N. V. Antonenko, R. V. Jolos et al., Phys. Rev. C 69, 054310 (2004).
- [16] B. Serot and J.D. Walecka, Adv. Nucl. Phys. 16, 1 (1986).
- [17] G.A. Lalazissis, P. Ring, Phys. Lett. B 427, 225 (1998).
- [18] P. -G. Reinhard, Rep. Prog. Phys. 52, 439(1989).
- [19] P. Ring, Prog. Part. Nucl. Phys. 37, 193(1996).
- [20] J. Meng, Nucl. Phys. A 635, 3(1998).
- [21] R. Brockmann and R. Machleidt, Phys. Rev. C 42, 1965(1990).
- [22] J. Meng and P. Ring, Phys. Rev. Lett. 77, 3963(1996).
- [23] J. Meng and P. Ring, Phys. Rev. Lett. 80, 460(1998).
- [24] A. Arima, M. Harvey, and K. Shimizu, Phys. Lett. B 30, 517(1969).
- [25] K. T. Hecht and A. Adler, Nucl. Phys. A 137, 129(1969).
- [26] J. N. Ginocchio, Phys. Rev. Lett. 78, 436(1997).
- [27] J. Meng, K. Sugawara-Tanabe, S. Yamaji, and A. Arima, Phys. Rev. C 59, 154 (1999).
- [28] J.-Y. Guo, R.-D. Wang, and X.-Z. Fang, Phys. Rev. C 72, 054319 (2005)
- [29] S. G. Zhou, J. Meng, and P. Ring, Phys. Rev. Lett. 91, 262501 (2003).
- [30] H. Madokoro, J. Meng, M. Matsuzaki, S.Yamaji, Phys.Rev. C 62, 061301(2000).
- [31] Z. Y. Ma, A. Wandelt, N. V. Giai, D. Vretenar, P. Ring, L. G. Cao, Nucl. Phys. A 703 222(2002).
- [32] J. König and P. Ring, Phys. Rev. Lett. 71, 3079(1993).
- [33] Y. Gambhir, P. Ring, A. Thimet, Ann. Phys. (N.Y.) 198, 132 (1990).
- [34] S.G.Zhou, J.Meng, P.Ring, Phys. Rev. C 68 (2003) 034323
- [35] P. Ring and P. Schuck, *The Nuclear Many Body Problem*, (Springer 1980).
- [36] G. A. Lalazissis, J. König, and P. Ring, Phys. Rev. C**55**, 540 (1997).
- [37] W. H. Long, J. Meng, N. V. Giai, and S. G. Zhou, Phys. Rev. C 69, 034319 (2004).
- [38] Y. Sugahara, and H. Toki, Nucl. Phys. A 579, 557 (1994).
- [39] M.M. Sharma, M.A. Nagarajan, and P. Ring, Phys. Lett. B312,377 (1993).
- [40] G. Audi and A. H. Wapstra, Nucl. Phys. A 595, 409(1995).